Pergamon

Int. J. Solids Structures Vol. 34, No. 11 pp. 1327–1341, 1997

0020-7683/97 $17.00 + .00

PII: S0020-7683(96)00103-5

# APPROXIMATE ELASTICITY SOLUTION FOR A LONG AND THICK LAMINATED CIRCULAR CYLINDRICAL SHELL OF REVOLUTION

K. CHANDRASHEKHARA and K. S. NANJUNDA RAO
Department of Civil Engineering, Indian Institute of Science, Bangalore-560 012, India

(*Received* 19 *August* 1995; *in revised form* 12 *May* 1996)

**Abstract**—An approximate three-dimensional elasticity solution is presented for an infinite, thick, orthotropic as well as laminated circular cylindrical shell of revolution subjected to distributed pinch load. The validity and the accuracy of the results of approximate solution has been established by comparing it with the results of an exact three-dimensional elasticity solution for single and multi-layered (hybrid) shell of revolution. Numerical results have been presented for cross-ply laminated (0/90/0 and 90/0/90) infinite circular cylindrical shell of revolution subjected to axisymmetric band and distributed pinch loads. These results have been compared with the classical and first-order shear deformation theories of Flugge and Donnell to assess the accuracy and limitations of the two-dimensional shell theories. © 1997 Elsevier Science Ltd. All rights reserved.

## 1. INTRODUCTION

Shell structures are not only aesthetical in appearance but also very efficient from structural point of view. With the advent of advanced fiber reinforced composite materials having many attractive properties like high strength to weight and stiffness to weight ratios, good corrosion and heat resistance and excellent fatigue strength, shells made of these materials have been extensively used in aerospace, civil, chemical, mechanical and marine industries. In the literature, several approaches have been made to study the static and dynamic response of composite shells. The approximate two-dimensional theories based on Kirchhoff–Love hypothesis of nondeformable normals or their refinements to include the effects of shear deformation and normal strain, initially proposed for isotropic shells have been extended to composite shells. In order to assess the accuracy and limitations of these two-dimensional (2D) shell theories, three-dimensional (3D) elasticity solutions are essential as they can be used as bench mark solutions. Recently Noor and Burton (1990) have systematically reviewed the available approaches and solutions based on 3D elasticity and 2D shell theories for the analysis of multilayered composite shells. Though in practice composite angle-ply/cross-ply laminated shells subjected to arbitrary loading are used, their governing 3D elasticity equations are very complicated and there are considerable mathematical difficulties in solving them. However, for a cross-ply laminate the basic governing equations of 3D elasticity (for shell problems) are a set of three, second-order partial differential equations with variable coefficients in terms of three displacements in the chosen cylindrical coordinate system and the solution of these equations is also quite involved. Several approaches are proposed in the literature for reducing these partial differential equations to ordinary differential equations with variable coefficient by assuming some functions in two directions satisfying the boundary and symmetry conditions. Using the displacement function approach the authors (Chandrashekhara & Rao, 1995) have recently presented an exact 3D elasticity solution for an infinitely long, thick and transversely isotropic circular cylindrical shell of revolution subjected to pinch load. However this solution is applicable only for unidirectional hybrid laminates (fibres oriented in the longitudinal direction only as in the case of interlaminar hybrid laminate). This method cannot be extended to more commonly used cross-ply laminated shells as the plane of isotropy is different for 0° and 90° lamina and the same form of displacement functions cannot be used for both the laminae. However many investigators in the past have attempted

to develop solutions to these variable coefficient differential equations using power series methods. The Frobenius method was first used by Srinivas (1974) for a simply-supported cross-ply laminated circular cylindrical shells and some numerical results were presented for free vibration problem. Later using the same approach numerical results for a simple static loading has been given by Varadan and Bhaskar (1991) for cross-ply laminated circular cylindrical shell of revolution. Recently Ren (1995) has used the power series method for analysis of anisotropic laminated circular cylindrical shells under axisymmetric loading. Even though the power series methods provide an exact solution, these methods have convergence difficulties particularly while dealing with highly discontinuous loads. It should be noted that this method has been employed by the above investigators to obtain solution to problems with simple loading only. As an alternative, an approximate elasticity solution under the assumption that $h_j/R_j \ll 1$ (where $h_j$ and $R_j$ are the thickness and middle surface radius of the $j$th lamina) and can be neglected was suggested by Soong (1970) and has been adopted by many investigators for static and free vibration analysis of composite laminated shells. The above assumption helps in reducing the ordinary differential equations with variable coefficient to one with constant coefficient, whose solution can be obtained by using a standard procedure. Chandrashekhara and Kumar (1993a, b) have used the above approach to obtain solution for finite laminated circular cylindrical shells subjected to both axisymmetric and asymmetric radial loads. An infinite orthotropic laminated cylindrical shell subjected to pinch load is a basic problem and to the authors knowledge there appears to be no 3D elasticity solution for the same. The solution to this problem would be specifically useful to study the local effects of highly discontinuous load on the stresses and deformations of the shell. Further the present solution would serve as a bench mark to verify the more general solutions based on other numerical methods. The main objectives of the present paper are to (i) develop an approximate 3D elasticity solution for long, thick, orthotropic and laminated circular cylindrical shell of revolution; (ii) establish the validity of the approximate 3D elasticity approach with respect to exact 3D elasticity solution developed earlier by the authors; (iii) assess the accuracy and limitations of 2D classical and shear deformation theories of Flugge and Donnell.

## 2. BASIC GOVERNING EQUATIONS

The global $(r, \theta, z)$ and local $(\bar{r}, \theta, z)$ coordinate system and the dimensions of the laminated shell of revolution are as shown in Fig. 1. The equilibrium equations in cylindrical

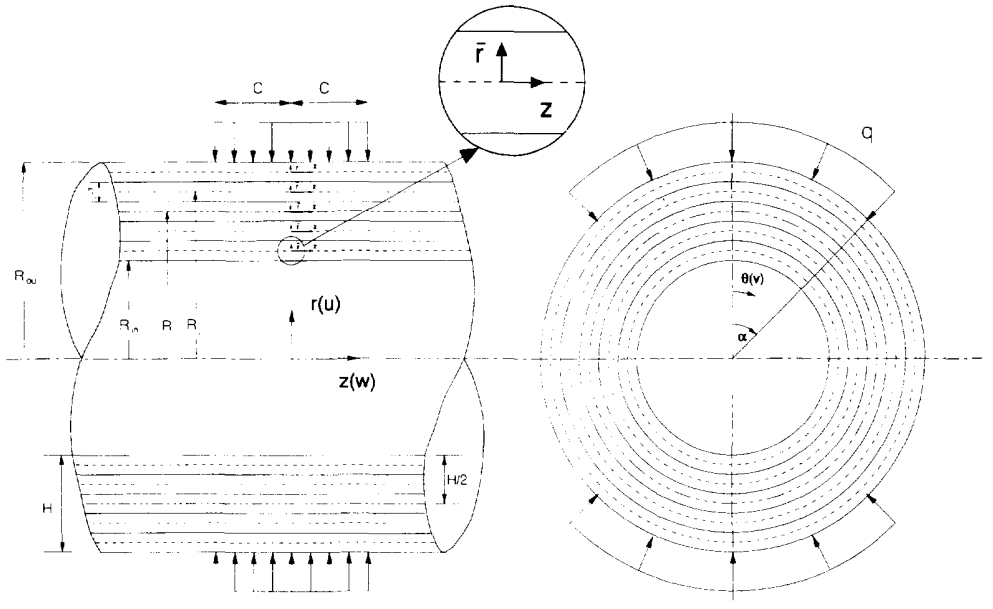


Fig. 1. Co-ordinate system and dimensions of laminated circular cylindrical shell of revolution.

coordinates $(r, \theta, z)$ (Lekhnitskii, 1963) can now be rewritten in terms of local coordinates $(\bar{r}, \theta, z)$ by shifting the origin to the middle surface of the lamina (Fig. 1) as,

$$\begin{aligned}
&\frac{\partial \sigma_r}{\partial \bar{r}} + \frac{1}{R_j + \bar{r}} \frac{\partial \tau_{r\theta}}{\partial \theta} + \frac{\partial \tau_{rz}}{\partial z} + \frac{\sigma_r - \sigma_\theta}{R_j + \bar{r}} = 0 \\
&\frac{\partial \tau_{r\theta}}{\partial \bar{r}} + \frac{1}{R_j + \bar{r}} \frac{\partial \sigma_\theta}{\partial \theta} + \frac{\partial \tau_{\theta z}}{\partial z} + \frac{2\tau_{\theta r}}{R_j + \bar{r}} = 0 \\
&\frac{\partial \tau_{rz}}{\partial \bar{r}} + \frac{1}{R_j + \bar{r}} \frac{\partial \tau_{\theta z}}{\partial \theta} + \frac{\partial \sigma_z}{\partial z} + \frac{\tau_{rz}}{R_j + \bar{r}} = 0.
\end{aligned} \tag{1}$$

Similarly the strain–displacement relations (Lekhnitskii, 1963) can be rewritten in local coordinates as,

$$\begin{aligned}
\varepsilon_r &= \frac{\partial u}{\partial \bar{r}} \\
\varepsilon_\theta &= \frac{u}{R_j + \bar{r}} + \frac{1}{R_j + \bar{r}} \frac{\partial v}{\partial \theta} \\
\varepsilon_z &= \frac{\partial w}{\partial z} \\
\gamma_{\theta z} &= \frac{\partial v}{\partial z} + \frac{1}{R_j + \bar{r}} \frac{\partial w}{\partial \theta} \\
\gamma_{rz} &= \frac{\partial u}{\partial z} + \frac{\partial w}{\partial \bar{r}} \\
\gamma_{r\theta} &= \frac{1}{R_j + \bar{r}} \frac{\partial u}{\partial \theta} + \frac{\partial v}{\partial \bar{r}} - \frac{v}{R_j + \bar{r}}
\end{aligned} \tag{2}$$

where $R_j$ is the middle surface radius of the $j$th lamina and $\bar{r}$ is measured from the middle surface of the lamina.

The stress–strain relations for an orthotropic lamina can be written as (Lekhnitskii, 1963)

$$\begin{Bmatrix} \sigma_r \\ \sigma_\theta \\ \sigma_z \\ \tau_{\theta z} \\ \tau_{rz} \\ \tau_{r\theta} \end{Bmatrix} = \begin{bmatrix} C_{11} & C_{12} & C_{13} & 0 & 0 & 0 \\ C_{12} & C_{22} & C_{23} & 0 & 0 & 0 \\ C_{13} & C_{23} & C_{33} & 0 & 0 & 0 \\ 0 & 0 & 0 & C_{44} & 0 & 0 \\ 0 & 0 & 0 & 0 & C_{55} & 0 \\ 0 & 0 & 0 & 0 & 0 & C_{66} \end{bmatrix} \begin{Bmatrix} \varepsilon_r \\ \varepsilon_\theta \\ \varepsilon_z \\ \gamma_{\theta z} \\ \gamma_{rz} \\ \gamma_{r\theta} \end{Bmatrix}. \tag{3}$$

In laminated composite shells commonly used in engineering applications, the thickness of each lamina is very small when compared with its middle surface radius. The implication of this assumption is that the ratio $(\bar{r}/R_j) \ll 1$ and hence can be neglected. Hence we can write

$$r = (R_j \pm \bar{r}) = R_j \left(1 \pm \frac{\bar{r}}{R_j}\right) \simeq R_j ; \partial r = \partial \bar{r}. \tag{4}$$

Using the above assumption (eqn (4)), the equilibrium equations in terms of displacements can be obtained, by substituting eqns (2) and (3) in eqn (1) as,

$$\begin{bmatrix} X_{11} & X_{12} & X_{13} \\ X_{21} & X_{22} & X_{23} \\ X_{31} & X_{32} & X_{33} \end{bmatrix} \begin{Bmatrix} u \\ v \\ w \end{Bmatrix} = \mathbf{0} \tag{5}$$

where,

$$X_{11} = C_{11}\left(\frac{\partial^2}{\partial \bar{r}^2} + \frac{1}{R_j}\frac{\partial}{\partial \bar{r}}\right) - \frac{C_{22}}{R_j^2} + \frac{C_{12}}{R_j^2} + C_{55}\frac{\partial^2}{\partial z^2} + C_{66}\frac{1}{R_j^2}\frac{\partial^2}{\partial \theta^2}$$

$$X_{12} = (C_{12} + C_{66})\frac{1}{R_j}\frac{\partial^2}{\partial \bar{r}\,\partial \theta} - (C_{22} + C_{66} - C_{12})\frac{1}{R_j^2}\frac{\partial}{\partial \theta}$$

$$X_{13} = (C_{13} - C_{23})\frac{1}{R_j}\frac{\partial}{\partial z} + (C_{13} + C_{55})\frac{1\partial^2}{\partial \bar{r}\,\partial z}$$

$$X_{21} = (C_{22} + 2C_{66})\frac{1}{R_j^2}\frac{\partial}{\partial \theta} + (C_{12} + C_{66})\frac{1}{R_j}\frac{\partial^2}{\partial \bar{r}\,\partial \theta}$$

$$X_{22} = C_{66}\left(\frac{\partial^2}{\partial \bar{r}^2} + \frac{1}{R_j}\frac{\partial}{\partial \bar{r}} - \frac{2}{R_j^2}\right) + C_{22}\frac{1}{R_j^2}\frac{\partial^2}{\partial \theta^2} + C_{44}\frac{\partial^2}{\partial z^2}$$

$$X_{23} = (C_{23} + C_{44})\frac{1}{R_j}\frac{\partial^2}{\partial z\,\partial \theta}$$

$$X_{31} = (C_{23} + C_{55})\frac{1}{R_j}\frac{\partial}{\partial z} + (C_{13} + C_{55})\frac{\partial^2}{\partial \bar{r}\,\partial z}$$

$$X_{32} = X_{23}$$

$$X_{33} = C_{55}\left(\frac{\partial^2}{\partial \bar{r}^2} + \frac{1}{R_j}\frac{\partial}{\partial \bar{r}}\right) + C_{44}\frac{1}{R_j^2}\frac{\partial^2}{\partial \theta^2} + C_{33}\frac{\partial^2}{\partial z^2}.$$

Any general loading acting on the shell can be split into axisymmetric and asymmetric (non-axisymmetric) parts. For the axisymmetric case the stresses, displacements and load are independent of the circumferential coordinate ($\theta$) and further the shear strains ($\gamma_{r\theta}, \gamma_{z\theta}$), shear stresses ($\tau_{r\theta}, \tau_{z\theta}$) and circumferential displacement ($v$) does not exist. As a result of the above simplifications the equilibrium equations for axisymmetric case will be two, second-order partial differential equations in terms of displacements ($u, w$) and can be written as,

$$\begin{bmatrix} \tilde{X}_{11} & \tilde{X}_{12} \\ \tilde{X}_{21} & \tilde{X}_{22} \end{bmatrix} \begin{Bmatrix} u \\ w \end{Bmatrix} = \mathbf{0}. \tag{6}$$

The expressions for $\tilde{X}_{11}, \tilde{X}_{12}, \tilde{X}_{21}, \tilde{X}_{22}$, can be obtained from the expressions given earlier for $X_{11}, X_{13}, X_{31}, X_{33}$ by deleting the terms containing derivatives with respect to $\theta$, respectively.

## 3. BOUNDARY AND CONTINUITY CONDITIONS

For an infinite laminated circular cylindrical shell of revolution made of '$N$' laminae the boundary conditions on the inner and outer surface of the shell can be written as (Fig. 1)

$$\sigma_r = \tau_{rz} = \tau_{r\theta} = 0, \quad \text{at } \bar{r} = -\frac{h_1}{2}$$

$$\sigma_r = -q(z,\theta), \quad \tau_{rz} = \tau_{r\theta} = 0, \quad \text{at } \bar{r} = \frac{h_N}{2} \tag{7}$$

where $h_1$ and $h_N$ are the thickness of the innermost and outermost lamina of the shell. Further the stresses and deformations should vanish as $z \to \infty$.

The continuity conditions of stresses and displacements to be enforced at any interface can be written as,

$$\begin{aligned}
[(\sigma_r)_{\bar{r}=h_j/2}]_j &= [(\sigma_r)_{\bar{r}=-h_{j+1}/2}]_{j+1} \\
[(\tau_{rz})_{\bar{r}=h_j/2}]_j &= [(\tau_{rz})_{\bar{r}=-h_{j+1}/2}]_{j+1} \\
[(\tau_{r\theta})_{\bar{r}=h_j/2}]_j &= [(\tau_{r\theta})_{\bar{r}=-h_{j+1}/2}]_{j+1} \\
[(u)_{\bar{r}=h_j/2}]_j &= [(u)_{\bar{r}=-h_{j+1}/2}]_{j+1} \\
[(v)_{\bar{r}=h_j/2}]_j &= [(v)_{\bar{r}=-h_{j+1}/2}]_{j+1} \\
[(w)_{\bar{r}=h_j/2}]_j &= [(w)_{\bar{r}=-h_{j+1}/2}]_{j+1}
\end{aligned} \tag{8}$$

where $h_j$ and $h_{j+1}$ are the thickness of $j$th and $(j+1)$th lamina.

For axisymmetric case only those stresses and displacements that exist need to be considered and hence the boundary conditions for this case reduce to

$$\sigma_r = \tau_{rz} = 0, \quad \text{at } \bar{r} = -\frac{h_1}{2}$$

$$\sigma_r = -q(z), \quad \tau_{rz} = 0, \quad \text{at } \bar{r} = \frac{h_N}{2} \tag{9}$$

and continuity conditions in respect of $\sigma_r$, $\tau_{rz}$, $u$ and $w$ need to be considered.

## 4. SOLUTION

The solution for axisymmetric and asymmetric (non-axisymmetric) cases has to develop independently as in the present method, the solution for asymmetric (non-axisymmetric) case does not reduce to one for axisymmetric case automatically. Hence the solution for the above two cases has been discussed separately.

### 4.1. *Asymmetric case (non-axisymmetric)*

The solution of the partial differential equations (eqn (5)) can be taken as,

$$\begin{aligned}
u &= \int_0^{\infty} \sum_{n=1}^{r} U(\bar{r}) \cos(2n\theta) \cos(\lambda z)\, d\lambda \\
v &= \int_0^{\infty} \sum_{n=1}^{r} V(\bar{r}) \sin(2n\theta) \cos(\lambda z)\, d\lambda \\
w &= \int_0^{\infty} \sum_{n=1}^{r} W(\bar{r}) \cos(2n\theta) \sin(\lambda z)\, d\lambda.
\end{aligned} \tag{10}$$

Substituting the expressions for $u$, $v$ and $w$ in eqn (5), results in three second-order ordinary differential equations in terms of radial coordinate ($\bar{r}$).

Assuming that,

$$\{U(\bar{r}), V(\bar{r}), W(\bar{r})\} = (U^*, V^*, W^*)\, e^{s\bar{r}} \tag{11}$$

where $U^*$, $V^*$ and $W^*$ are constants.

Substituting now eqns (10) and (11) in eqn (5) will result in a system of following three algebraic equations.

$$\begin{bmatrix} \{b_1(s^2+s)+b_2\} & \{b_3 s - b_4\} & \{b_5 s + b_6\} \\ \{b_7 - b_3 s\} & \{b_8(s^2+s)+b_9\} & \{b_{10}\} \\ \{-b_5 s + b_{11}\} & \{b_{10}\} & \{b_{12}(s^2+s)+b_{13}\} \end{bmatrix} \begin{Bmatrix} U^* \\ V^* \\ W^* \end{Bmatrix} = 0. \tag{12}$$

The expressions for $b_1, b_2, \ldots, b_{13}$ are given in the Appendix. For nontrivial solution of the above system of algebraic equations (eqn 12), the determinant of the coefficient matrix should vanish, which results in the following polynomial equation.

$$As^6 + Bs^5 + Cs^4 + Ds^3 + Es^2 + Fs + G = 0 \tag{13}$$

where the coefficients $A$–$G$ depend on the stiffness constants ($C_{ij}$), Fourier harmonic ($n$), $\lambda$ and the middle surface radius of the lamina under consideration. The six roots of the above polynomial (eqn (13)) can be obtained by any standard numerical procedure. They can be either all real or all complex or a combination of real and complex roots. The general solution for $U$, $V$ and $W$ can then be written down depending on the nature of these roots.

*Case* 1. If all the roots $s_k$ ($k = 1, \ldots, 6$) are real, the solution can be written, as

$$U(\bar{r}) = \sum_{k=1}^{6} U_k(\bar{r})$$

$$V(\bar{r}) = \sum_{k=1}^{6} P_k U_k(\bar{r})$$

$$W(\bar{r}) = \sum_{k=1}^{6} Q_k U_k(\bar{r}) \tag{14}$$

where $U_k(\bar{r}) = a_k e^{s_k \bar{r}}$ and $a_k$ ($k = 1, 2, \ldots, 6$) are the unknown constants. The expressions for $P_k$ and $Q_k$ are given in the Appendix.

*Case* 2. If all the roots are complex, then

$$s_k^{(1)}, s_k^{(2)} = (\xi_k \pm i\eta_k) \quad (k = 1, 2, 3).$$

The solution can be written as

$$U(\bar{r}) = \sum_{k=1}^{3} [a_k(\cos \eta_k \bar{r}) - a_{k+3}(\sin \eta_k \bar{r})]\, e^{\xi_k \bar{r}}$$

$$V(\bar{r}) = \sum_{k=1}^{3} [a_k\{K_k \cos \eta_k \bar{r} - M_k \sin \eta_k \bar{r}\} - a_{k+3}\{M_k \cos \eta_k \bar{r} + K_k \sin \eta_k \bar{r}\}]\, e^{\xi_k \bar{r}}$$

$$W(\bar{r}) = \sum_{k=1}^{3} [a_k\{L_k \cos \eta_k \bar{r} - N_k \sin \eta_k \bar{r}\} - a_{k+3}\{N_k \cos \eta_k \bar{r} + L_k \sin \eta_k \bar{r}\}]\, e^{\xi_k \bar{r}} \tag{15}$$

where $a_k$ ($k = 1, 2, \ldots, 6$) are the unknown constants. The expressions for $K_k$, $L_k$, $M_k$ and $N_k$ for complex conjugate roots are given in the Appendix.

*Case* 3. If some roots are real and some are complex, the solution would be a combination of case 1 and 2 discussed above. The expressions for stress components can be obtained by using eqn (14) or eqn (15) (as the case may be), in eqns (10), (2) and (3). For a laminated shell consisting of '$N$' lamina, there will be '$6N$' unknown constants, which can be determined using three boundary conditions on each of the inner and outer surface of the shell (eqn (7)) and continuity conditions (eqn (8)) at $(N-1)$ interfaces. After evaluating the constants the displacements and stresses can be computed by back substitution for each lamina.

4.2. *Axisymmetric case*

The solution of the partial differential equations (eqn (6)) for axisymmetric case can be taken as,

$$u = \int_0^\infty U(\bar{r})\cos(\lambda z)\,\mathrm{d}\lambda$$

$$w = \int_0^\infty W(\bar{r})\sin(\lambda z)\,\mathrm{d}\lambda. \tag{16}$$

Substituting the above expressions for $u$ and $w$ in eqn (6), results in two, second-order ordinary differential equations in terms of radial coordinate $(\bar{r})$. The solution for $U(\bar{r})$ and $W(\bar{r})$ can be assumed in the following form,

$$\{U(\bar{r}), W(\bar{r})\} = (U^*, W^*)\,\mathrm{e}^{s\bar{r}} \tag{17}$$

where $U^*$, $W^*$ are constants. Substituting eqns (16) and (17) in eqn (6) will result in a system of two algebraic equations.

$$\begin{bmatrix} C_{11}(s^2+s)+C_{12}-C_{22}-C_{55}(\lambda R_j)^2 & (C_{13}+C_{55})\lambda R_j s+(C_{13}-C_{23})\lambda R_j \\ -(C_{55}+C_{13})\lambda R_j s-(C_{23}+C_{55})\lambda R_j & C_{55}(s^2+s)-C_{33}(\lambda R_j)^2 \end{bmatrix} \begin{Bmatrix} U^* \\ W^* \end{Bmatrix} = 0. \tag{18}$$

For non-trivial solution of the above system of equations (eqn 18) the determinant of the coefficient matrix should vanish, which results in the following polynomial equation

$$\tilde{A}s^4+\tilde{B}s^3+\tilde{C}s^2+\tilde{D}s+\tilde{E}=0. \tag{19}$$

The general solution for $u$ and $w$ can be obtained depending on the nature of the roots of the above polynomial equation, similar to the asymmetric case discussed earlier. The stresses and displacements can be computed after evaluating the unknown constants by making use of surface boundary conditions and continuity conditions (eqn (9)) as explained earlier for asymmetric case. The results for a general load (like for example pinch load) can be obtained by superposing the results of the axisymmetric case over the corresponding results of the asymmetric (non-axisymmetric) case.

## 5. NUMERICAL RESULTS AND DISCUSSION

A detailed numerical study has been made to establish the range of validity of the present approximate 3D elasticity solution by comparing its results with the results of the exact 3D elasticity solution proposed earlier by the authors (Chandrashekhara & Rao, 1995) for infinite single and hybrid laminated circular cylindrical shell of revolution. Later results are presented for cross-ply laminated shell of revolution for various shell thicknesses with a view to assess and establish the range of applicability of two-dimensional shell

theories. For the purpose of numerical results two materials, namely E–glass–epoxy (M1) and high modulus GRP (M2) have been considered. The properties of these materials are as follows.

| Material | $E_z$ (GPa) | $E_\theta$ (GPa) | $G_{rz}$ (GPa) | $G_{r\theta}$ (GPa) | $\mu_{r\theta}$ | $\mu_{z\theta}$ |
|---|---|---|---|---|---|---|
| E–Glass–epoxy [M1] | 43.8 | 12.42 | 4.7 | 4.5 | 0.37 | 0.24 |
| High modulus GRP [M2] | 172.38 | 6.90 | 3.45 | 1.4 | 0.25 | 0.25 |

For a transversely isotropic material the shear modulus $G_{r\theta}$ is given by

$$G_{r\theta} = \frac{E_\theta}{2(1+\mu_{r\theta})}.$$

Numerical results for the following problems are presented here:

(i) Infinite single-layer transversely isotropic circular cylindrical shell of revolution made of material M2 with fibres in the longitudinal ($z$) direction subjected to (a) axisymmetric band load ($\bar{c} = c/R = 0.025$) and (b) distributed pinch load.

(ii) Infinite transversely isotropic 3-ply hybrid laminated circular cylindrical shell of revolution with fibres in the longitudinal ($z$) direction in all the three layers, but with material M2 at top and bottom laminae and material M1 for middle lamina with unequal thickness plies, in the ratio of 1:2:3 from top to bottom subjected to (a) axisymmetric band load and (b) distributed pinch load.

(iii) Infinite orthotropic cross-ply laminated circular cylindrical shell of revolution made of material M2 (a) with fibres in the longitudinal ($z$) direction in top and bottom plies and in transverse ($\theta$) direction in the middle ply (0/90/0) (b) with fibres in transverse ($\theta$) direction in top and bottom plies and in the longitudinal ($z$) direction in the middle ply (90/0/90), all plies of equal thickness ($h = H/3$), subjected to axisymmetric band load ($\bar{c} = c/R = 0.025$) and radial distributed pinch load.

### 5.1. *Types of load considered*

(*a*) *Axisymmetric band load.* The axisymmetric band load $q(z)$ acting on the outer surface ($r = R_{ou}$) of the shell of revolution can be expressed as

$$q(z) = \int_0^\infty q(\lambda)\cos(\lambda z)\,\mathrm{d}\lambda$$

where,

$$q(\lambda) = \left(\frac{2q}{\pi}\right)\left(\frac{\sin \lambda c}{\lambda}\right).$$

(*b*) *Distributed pinch load.* The radial distributed pinch load $q(z,\theta)$ acting on the outer surface ($r = R_{ou}$) of the shell of revolution (Fig. 1) can be expressed as

$$q(z,\theta) = \int_0^\infty \sum_{n=0}^{\infty} q_{zn}\cos(2n\theta)\cos(\lambda z)\,\mathrm{d}\lambda$$

where,

$$q_{zn} = \left(\frac{4q\alpha}{\pi^2}\right)\left(\frac{\sin \lambda c}{\lambda}\right) \quad \text{for } n = 0 \text{ (axisymmetric)} \quad \text{and}$$

$$q_{zn} = \left(\frac{8q}{\pi^2}\right)\left(\frac{\sin 2n\alpha}{2n}\right)\left(\frac{\sin \lambda c}{\lambda}\right) \quad \text{for } n \geqslant 0 \text{ (non-axisymmetric)}$$

where $2c$ and $2\alpha$ are the linear and angular dimensions of the area over which the load is acting. The dimensions of the radial load considered are $c/R = 0.025$ and $\alpha = 1/8$ radians acting as shown in Fig. 1.

The stresses and displacements presented in tables and figures are non-dimensionalized as follows:

$$(\bar{\sigma}_\theta, \bar{\sigma}_z, \bar{\tau}_{rz}) = \frac{1}{q}(\sigma_\theta, \sigma_z, \tau_{rz})$$

$$(\bar{u}) = \frac{E}{qR}(u)$$

where $E$ is taken as 10 GPa. In the figures, thickness coordinate is non-dimensionalized with respect to outer radius ($R_{ou}$) of the shell.

The infinite integrals for calculating displacements and stresses were evaluated numerically using five point interpolation formula [Zurmuhl (1965)] both for elasticity and shell theory solutions. For elasticity solution convergence of infinite integrals and Fourier series has been established by a detailed numerical study and it has been found that for the distributed pinch load considered here good convergence can be obtained by considering the upper limit of integration as 400 and number of terms ($n$) in the Fourier series upto 45. For the case of axisymmetric band load good convergence can be obtained by considering the upper limit of integration as 400.

In order to establish the range of validity of approximate solution with respect to exact solution numerical results are presented in Tables 1 and 2 for an infinite single and hybrid

Table 1. Comparative study of results of exact and approximate 3D analysis of single layer transversely isotropic circular cylindrical shell of revolution of material M2 subjected to axisymmetric band load ($\bar{c} = 0.025$) for various shell thickness

| | $H/R$ | | | | | | | |
|---|---|---|---|---|---|---|---|---|
| displacement/ | 0.05 | | 0.10 | | 0.20 | | 0.50 | |
| stress↓ | exact | approx. | exact | approx. | exact | approx. | exact | approx. |
| $-\bar{u}(R, 0, 0)$ | 2.13999 | 2.15204 | 0.83146 | 0.84687 | 0.34431 | 0.35517 | 0.12244 | 0.12617 |
| $\bar{\sigma}_z(R_{ou}, 0, 0)$ | −14.83103 | −14.75919 | −8.16968 | −8.22468 | −5.69818 | −6.02648 | −4.53576 | −5.24641 |
| $\bar{\sigma}_z(R_{in}, 0, 0)$ | 12.93481 | 12.75873 | 5.03483 | 4.92099 | 1.92212 | 1.86144 | 0.61012 | 0.49960 |
| $-\bar{\sigma}_\theta(R_{ou}, 0, 0)$ | 1.89639 | 1.90481 | 0.94016 | 0.95298 | 0.59258 | 0.60814 | 0.41332 | 0.46492 |
| $-\bar{\sigma}_\theta(R_{in}, 0, 0)$ | 1.42951 | 1.36339 | 0.58505 | 0.53609 | 0.26980 | 0.22483 | 0.12860 | 0.07855 |
| $\bar{\tau}_{rz}(R, 0, 0.025R)$ | 0.50095 | 0.49921 | 0.20406 | 0.20086 | 0.068719 | 0.067538 | 0.015054 | 0.012335 |

Table 2. Comparative study of results of exact and approximate 3D analysis of hybrid laminated circular cylindrical shell of revolution made of three laminae (M2, M1, M2) of unequal thickness (1:2:3) subjected to axisymmetric band load ($\bar{c} = 0.025$) for various shell thickness

| | $h_1/R_1(H/R)$ | | | | | | | |
|---|---|---|---|---|---|---|---|---|
| displacement/ | 0.0253(0.05)* | | 0.0513(0.1)* | | 0.105(0.2)* | | 0.1917(0.35)* | |
| stress↓ | exact | approx. | exact | approx. | exact | approx. | exact | approx. |
| $-\bar{u}(R, 0, 0)$ | 1.82898 | 1.82766 | 0.71605 | 0.71439 | 0.29863 | 0.29722 | 0.15548 | 0.15429 |
| $\bar{\sigma}_z(R_{ou}, 0, 0)$ | −14.89178 | −14.64548 | −7.74305 | −7.59253 | −5.55801 | −5.52760 | −4.84534 | −5.10086 |
| $\bar{\sigma}_z(R_{in}, 0, 0)$ | 11.84817 | 11.58130 | 4.65761 | 4.44525 | 1.83593 | 1.67569 | 0.87818 | 0.75546 |
| $-\bar{\sigma}_\theta(R_{ou}, 0, 0)$ | 1.67578 | 1.64697 | 0.84868 | 0.82694 | 0.55353 | 0.53710 | 0.44875 | 0.44775 |
| $-\bar{\sigma}_\theta(R_{in}, 0, 0)$ | 1.21338 | 1.16615 | 0.49977 | 0.46147 | 0.23086 | 0.19740 | 0.13929 | 0.10673 |
| $\bar{\tau}_{rz}(R, 0, 0.025R)$ | 0.56469 | 0.55834 | 0.25680 | 0.24710 | 0.09875 | 0.08716 | 0.04025 | 0.03098 |

*Values in the brackets are ratio of thickness of laminate ($H$) to the middle surface radius of the laminate ($R$).

Table 3. Comparative study of results of exact and approximate 3D analysis for a single (M2) and hybrid laminated (M2, M1, M2) shell of revolution subjected to distributed pinch load (Fig. 1).

| Displacement/stress | | $-\bar{u}(R, 0, 0)$ | $\bar{\sigma}_z(R_{ou}, 0, 0)$ | $\bar{\sigma}_\theta(R_{ou}, 0, 0)$ |
|---|---|---|---|---|
| Single shell | Exact | 0.5717 | −6.1368 | −0.7609 |
| $(H/R = 0.2)$ | Approx. | 0.5776 | −5.6869 | −0.7052 |
| Hybrid laminate | Exact | 0.1573 | −5.0285 | −0.4862 |
| $(H/R = 0.35, h_1/R_1 = 0.19)$ | Approx. | 0.1659 | −4.8716 | −0.4599 |

laminated shell of revolution for various shell thicknesses. In Table 1 comparison of exact and approximate solution results for single layer transversely isotropic shell of revolution made of material M2 and subjected to axisymmetric band load is presented. In all four ratios of shell thickness to mean radius varying from 0.05 to 0.5 have been considered. It can be observed from this table that the results of approximate solution are in good agreement with the exact solution for $H/R$ upto 0.2 with a maximum percentage error of 5.76 in respect of longitudinal stress on the outer surface of shell directly under the load. Hence it may be concluded that the present approximate solution can be extended for analysis of thick laminated shell, provided the ratio of thickness to mean radius of each lamina is $\leqslant 0.2$. It is pertinent to point out that with this limitation on ratio of thickness to mean radius of the lamina, even very thick laminated shells can be analyzed using the approximate solution. This could be seen from the results presented in Table 2 for hybrid laminated shell of revolution that the approximate solution results are in good agreement with exact solution even when $H/R = 0.35$. In the above table $h_1$ and $R_1$ are the thickness and mean radius of the innermost lamina, for which the ratio of thickness to mean radius will be the highest. A detailed study, similar to the axisymmetric case, was made to establish the limitation of the approximate solution for pinch load case and only some typical results are presented here. In Table 3, a comparison of the results of exact and approximate 3D analysis for single shell with $H/R = 0.2$ made of material M2 and hybrid laminated shell made of three laminae (M2, M1, M2) of unequal thickness (1:2:3) with $H/R = 0.35$ $(h_1/R_1 = 0.19)$ subjected to distributed pinch load are presented. It can be seen from this table that the maximum error in approximate solution in respect of all stresses and displacements is less than 10%.

To study the effect of shell thickness on the stresses and displacements, for cross-ply laminates (0/90/0 and 90/0/90) three ratios of inner to outer radius of shell $(R_{in}/R_{ou})$ namely, 0.9512, 0.9048 and 0.8182 (with corresponding thickness to mean radius ratios of the laminate $(H/R) = 0.05$, 0.1 and 0.2, respectively) have been considered.

Numerical results based on classical and first-order shear deformation shell theories according to Flugge (CSTF and FSDTF) and Donnell (CSTD and FSDTD) have also been obtained for cross-ply laminated shell. They are examined by comparing with the present approximate elasticity solution to assess the accuracy and limitations of shell theories. Figures 2–7 shows the variation of nondimensionalized radial displacement $(\bar{u})$, longitudinal $(\bar{\sigma}_z)$ and circumferential $(\bar{\sigma}_\theta)$ stresses and transverse shear stress $(\bar{\tau}_{rz})$ over the thickness of the shell. The results obtained from approximate elasticity solution is indicated in these figures as 'ET'.

The variation of radial displacement over the shell thickness for shell of revolution subjected to axisymmetric band and pinch loads for different $H/R$ ratios and lamination schemes for a typical material M2 is presented in Figs 2 and 4, respectively. It may be seen from these figures that the elasticity theory indicates the radial displacement to be constant over the shell thickness for $H/R = 0.05$ while for $H/R \geqslant 0.1$ it is not constant for both the lamination schemes considered in the present study. However, it can be seen that shell theories always underpredict radial displacement for all $H/R$ ratios and lamination schemes considered here. For example the magnitude of radial displacement at middle surface of laminate (90/0/90) as predicted by CST of Flugge and Donnell are 18% and 36% lower than those obtained by approximate elasticity theory for $H/R = 0.05$, while for $H/R = 0.2$ the error is 64% and 74%, respectively. Incorporation of first-order shear deformation in

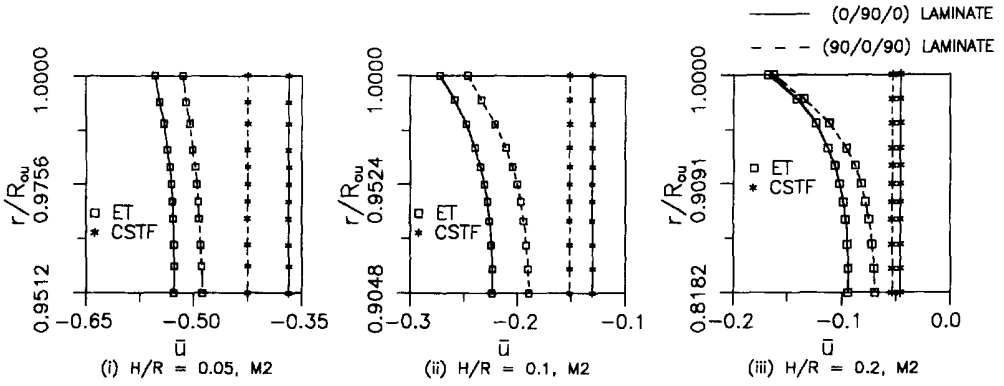


Fig. 2. Variation of radial displacement ($\bar{u}$) over the thickness of the shell at $z/R = 0$ for axisymmetric band load.

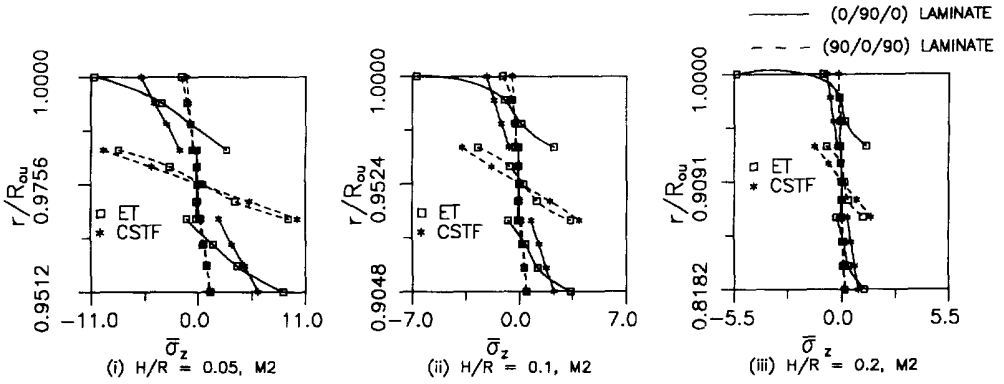


Fig. 3. Variation of longitudinal stress ($\bar{\sigma}_z$) over the thickness of the shell at $z/R = 0$ for axisymmetric band load.

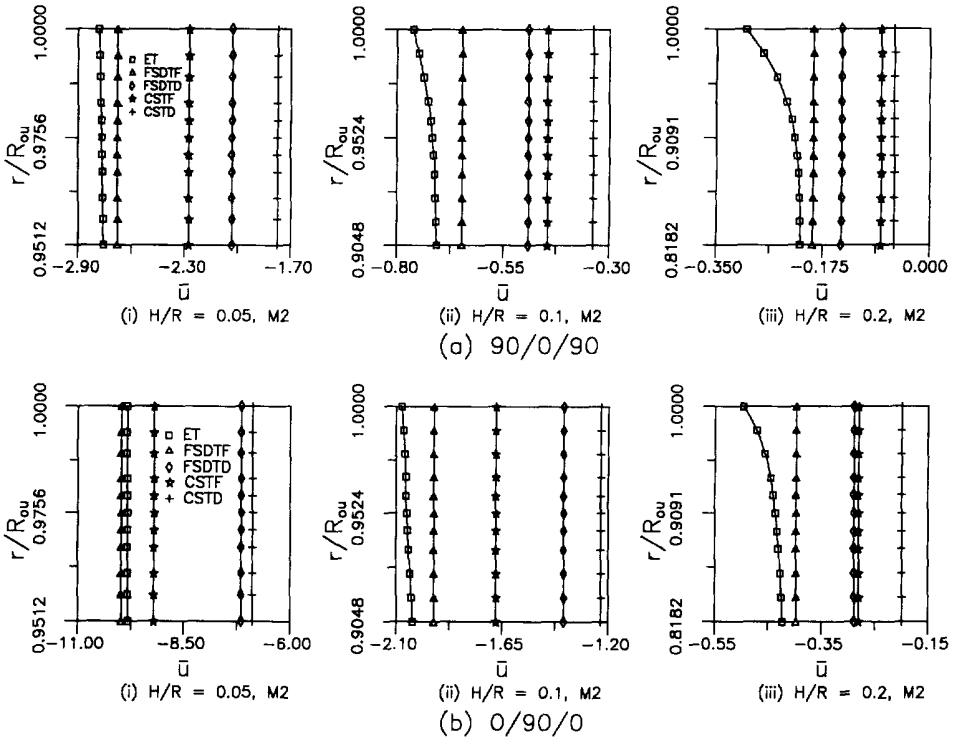


Fig. 4. Variation of radial displacement ($\bar{u}$) over the thickness at $z/R = 0$ and $\theta = 0$ for distributed pinch load.

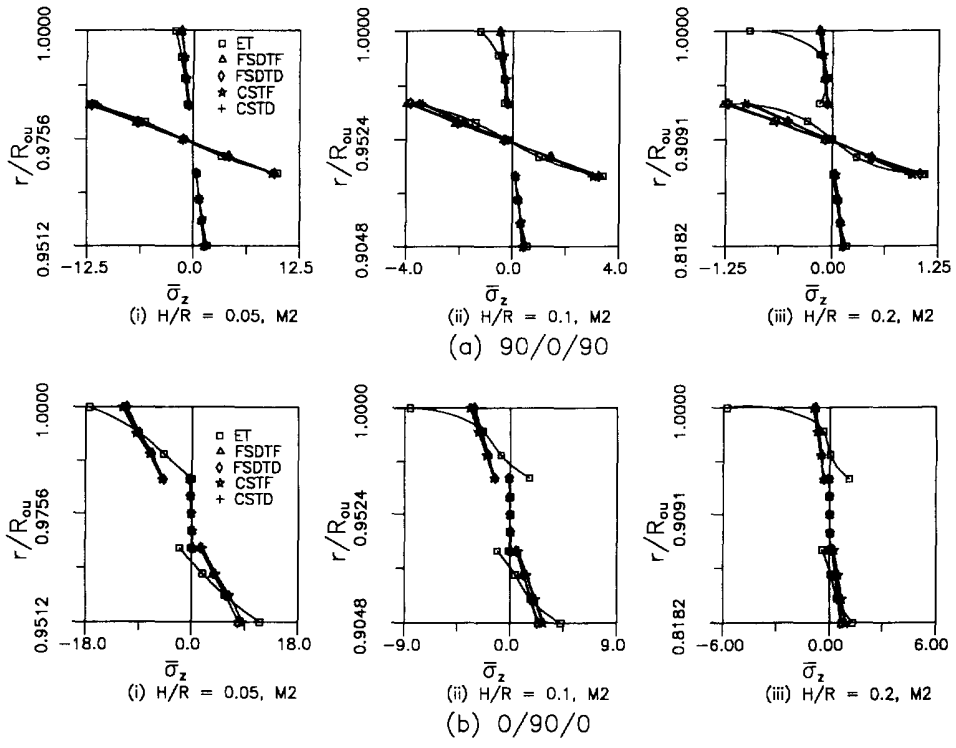


Fig. 5. Variation of longitudinal stress ($\bar{\sigma}_z$) over the thickness at $z/R = 0$ and $\theta = 0$ for distributed pinch load.

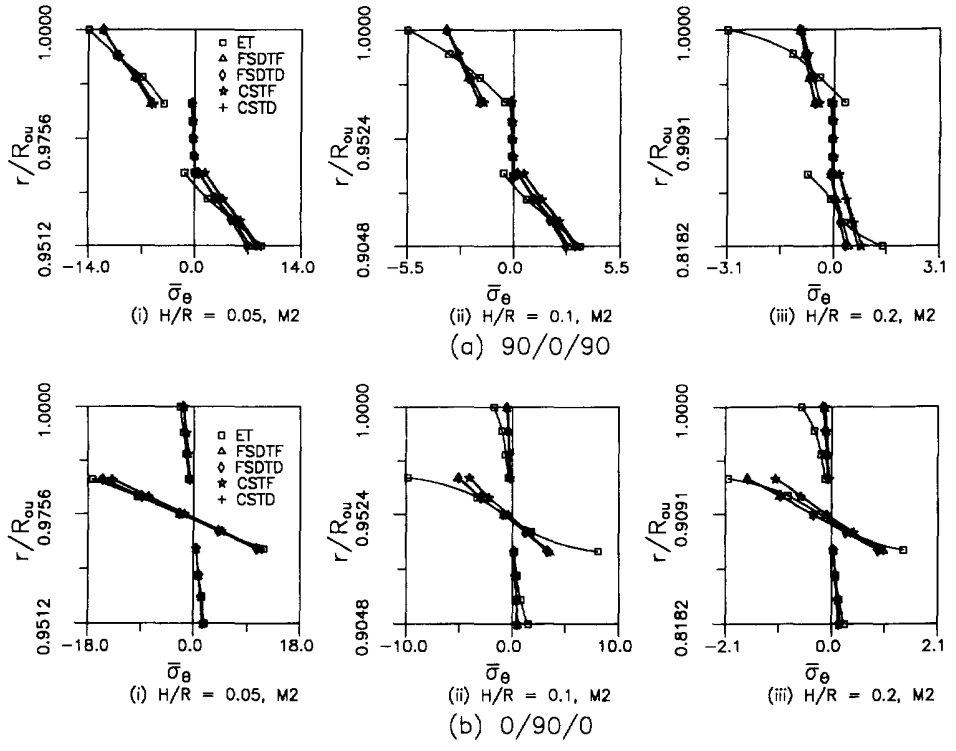


Fig. 6. Variation of circumferential stress ($\bar{\sigma}_\theta$) over the thickness at $z/R = 0$ and $\theta = 0$ for distributed pinch load.

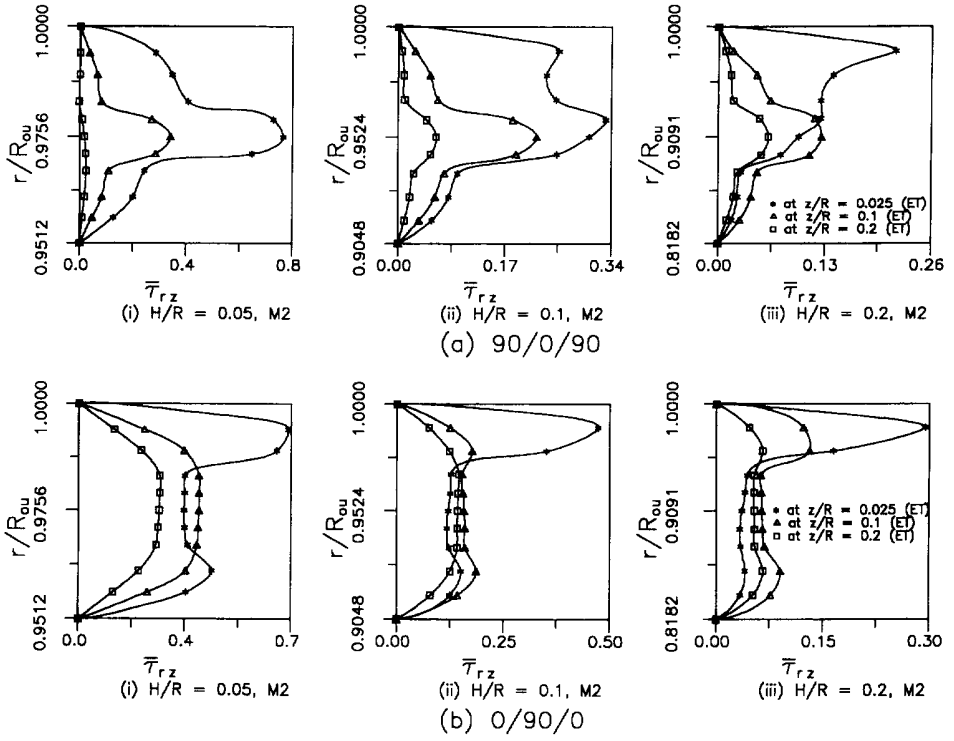


Fig. 7. Variation of transverse shear stress ($\bar{\tau}_{rz}$) over the thickness at $\theta = 0$ for distributed pinch load.

classical shell theories improves the prediction of radial displacement. For example for $H/R = 0.2$, FSDT of Flugge and Donnell underpredict radial displacement to the extent of 14% and 35%, respectively. Further it can be seen from Fig. 2 that the difference between elasticity solution results and classical shell theory results of Flugge is higher in the case of a laminate having more of 0° laminae than 90° laminae for all the $H/R$ ratios considered. The variation of longitudinal stress over the thickness of the shell for different thickness and lamination schemes is shown in Figs 3 and 5. It can be seen from these figures that the variation of longitudinal stress is almost linear for $H/R = 0.05$ and 90/0/90 laminate, but nonlinear for $H/R \geqslant 0.1$. Further it can be observed that the shell theory results deviate considerably from elasticity results for 0/90/0 laminate even for a thin shell ($H/R = 0.05$). It can also be seen that the magnitude of longitudinal stress is very small in 90° lamina compared with 0° lamina. The variation of circumferential stress over the thickness of the shell for different thickness and lamination schemes is shown in Fig. 6. It can be seen from this figure that the variation of circumferential stress is almost linear for $H/R = 0.05$, but nonlinear for $H/R \geqslant 0.1$. The magnitude of circumferential stress predicted by shell theories at the interfaces of the laminate are considerably different from those predicted by the present approximate 3D elasticity theory. This is because in shell theories the laminate is taken as an equivalent orthotropic shell whereas in elasticity solution the properties of each individual lamina is considered in the analysis. It can also be seen that the magnitude of the circumferential stress is very small in 0° lamina compared with 90° lamina. The variation of transverse shear stress over the shell thickness (elasticity solution only) for different thickness ratios and lamination schemes at different sections in the longitudinal direction, are shown in Fig. 7. It can be seen from this figure that at sections far away from the load ($z/R \geqslant 0.1$) the shear stress distribution is parabolic for thin ($H/R = 0.05$) laminated shells (0/90/0). For thick ($H/R \geqslant 0.1$) laminated shells (0/90/0) the distribution of shear stress is not parabolic even at sections far away from the load ($z/R \geqslant 0.1$). In the case of (90/0/90) laminated shell even though the shear stress distribution is not parabolic, the maximum shear stress is at the middle surface of the shell unlike in (0/90/0) laminate where the maximum shear stress occurs some where near the outer surface of the shell. Further it can

be seen that shear stress distribution is far from parabolic at the point of discontinuity of load ($z/R = 0.025$).

## 6. CONCLUSIONS

From the above discussion it can be concluded that the magnitude and variation of displacement and stresses are affected by the shell thickness, lamination scheme and nature of loading. The approximate 3D elasticity solution presented here predicts reasonably accurate results (compared with exact solution for a single and layered transversely isotropic shell) for $H/R$ upto 0.2. From the results presented for hybrid laminated shell it may be concluded that approximate solution can be used to analyse thick laminates, provided the thickness to mean radius ratio of individual lamina is $\leqslant 0.2$. Comparison of results obtained by shell theories with respect to approximate elasticity solution for cross-ply laminates brings out the following points. The variation of longitudinal and circumferential stress over the shell thickness is non-linear for thick shells ($H/R \geqslant 0.1$). The variation of radial displacement over the shell thickness is constant for $H/R = 0.05$ and is not constant for $H/R \geqslant 0.1$. All shell theories underpredict the radial displacement and classical shell theory of Donnell gives unacceptable results even for a thin shell ($H/R = 0.05$). In general it may be concluded that, incorporation of shear deformation over an accurate theory like Flugge can give better results than on an approximate theory like Donnell. The present investigation serves as a bench mark elasticity solution, which would be useful to verify the accuracy and limitations of approximate 2D shell theories and the solutions based on other numerical methods.

*Acknowledgement*—The first author gratefully acknowledges the financial support provided by AICTE, New Delhi, India.

## REFERENCES

Chandrashekhara, K. and Kumar, B. S. (1993a) Static analysis of a thick laminated circular cylindrical shell subjected to axisymmetric load. *Composite Structures* **23,** 1–9.

Chandrashekhara, K. and Kumar, B. S. (1993b) Static analysis of thick laminated circular cylindrical shells. *ASME Journal of Pressure Vessel Technology* **115,** 193–200

Chandrashekhara, K. and Nanjunda Rao, K. S. (1995) Static analysis of a long and thick orthotropic circular cylindrical shell of revolution. *Archive of Applied Mechanics* (Ingenieur Archiv) **65,** 425–436.

Lekhnitskii, S. G. (1963) *Theory of Elasticity of an Anisotropic Elastic Body* (translated from Russian). Holden-Day, San Francisco, CA.

Noor, A. K. and Burton, W. Scott (1990) Assessment of computational models for multi-layered composite shells. *ASME Applied Mechanics Review* **43,** 67–96.

Ren, J. G. (1995) Analysis of laminated circular cylindrical shells under axisymmetric loading. *Composite Structures* **30,** 271–280.

Soong, T. V. (1970) A subdivisional method for linear system. In *Proceedings 11th AIAA/ASME Structures, Structural Dynamics and Materials Conferences*, pp. 211–223.

Srinivas, S. (1974) Analysis of laminated, composite circular cylindrical shells with general boundary conditions. NASA Technical Report, NASA TR R-412. Washington, DC.

Varadan, T. K. and Bhaskar, K. (1991) Bending of laminated orthotropic cylindrical shells—an elasticity approach. *Composite Structures* **17,** 141–156.

Zurmuhl, (1965) *Praktische Mathematik fur Ingenieure und Physiker*. Springer, Berlin.

## APPENDIX A

$$b_1 = C_{11}; b_2 = C_{12} - C_{22} - C_{55}(\lambda R_j)^2 - (2n)^2 C_{66}; b_3 = (C_{12} + C_{66})2n$$

$$b_4 = 2n(C_{66} - C_{12} + C_{22}); b_5 = (C_{13} + C_{55})\lambda R_j; b_6 = (C_{13} - C_{23})\lambda R_j$$

$$b_7 = -2n(C_{22} + 2C_{66}); b_8 = C_{66}; b_9 = -[2C_{66} + (2n)^2 C_{22} + C_{44}(\lambda R_j)^2]$$

$$b_{10} = -2n(C_{23} + C_{44})\lambda R_j; b_{11} = -(C_{23} + C_{55})\lambda R_j; b_{12} = C_{55}$$

$$b_{13} = -[(2n)^2 C_{44} + C_{33}(\lambda R_j)^2].$$

For real roots:

$$P_k = \frac{(b_7 - b_3 s_k)(b_5 s_k + b_6) - [b_1(s_k^2 + s_k) + b_2]b_{10}}{(b_3 s_k - b_4)b_{10} - [b_8(s_k^2 + s_k) + b_9](b_5 s_k + b_6)}$$

$$Q_k = \frac{[b_1(s_k^2 + s_k) + b_2][b_8(s_k^2 + s_k) + b_9] - (b_7 - b_3 s_k)(b_3 s_k - b_4)}{(b_3 s_k - b_4)b_{10} - [b_8(s_k^2 + s_k) + b_9](b_5 s_k + b_6)}$$

$$k = 1, 2, \ldots, 6.$$

For complex roots:

$$K_k = (e_1 e_3 + e_2 e_4)/(e_1^2 + e_2^2);\ L_k = (e_1 e_5 + e_2 e_6)/(e_1^2 + e_2^2)$$

$$M_k = (e_1 e_4 - e_2 e_3)/(e_1^2 + e_2^2);\ N_k = (e_1 e_6 - e_2 e_5)/(e_1^2 + e_2^2)$$

where

$$e_1 = (b_3 b_{10} - b_9 b_5)\xi_k - b_4 b_{10} - b_9 b_6 - (b_8 b_5 \xi_k + b_8 b_6)(\xi_k^2 - \eta_k^2 + \xi_k) + b_8 b_5 (2\xi_k \eta_k + \eta_k)\eta_k$$

$$e_2 = (b_3 b_{10} - b_9 b_5)\eta_k - (b_8 b_5 \xi_k + b_8 b_6)(2\xi_k \eta_k + \eta_k) - b_8 b_5 (\xi_k^2 - \eta_k^2 + \xi_k)\eta_k$$

$$e_3 = (b_7 b_5 - b_3 b_6)\xi_k - (b_3 b_5)(\xi_k^2 - \eta_k^2) - [b_1(\xi_k^2 - \eta_k^2 + \xi_k) + b_2]b_{10} + b_7 b_6$$

$$e_4 = (b_7 b_5 - b_3 b_6)\eta_k - 2b_3 b_5 \xi_k \eta_k - [b_1(2\xi_k \eta_k + \eta_k)]b_{10}$$

$$e_5 = [b_1(\xi_k^2 - \eta_k^2 + \xi_k) + b_2][b_8(\xi_k^2 - \eta_k^2 + \xi_k) + b_9] - b_1 b_8 (2\xi_k \eta_k + \eta_k)^2 - (b_7 b_3 + b_5 b_4)\xi_k + b_3^2(\xi_k^2 - \eta_k^2) + b_7 b_4$$

$$e_6 = [b_1(\xi_k^2 - \eta_k^2 + \xi_k) + b_2][b_8(2\xi_k \eta_k + \eta_k)] + [b_1(2\xi_k \eta_k + \eta_k)][b_8(\xi_k^2 - \eta_k^2 + \xi_k) + b_9] - (b_7 b_3 + b_5 b_4)\eta_k + 2b_3 \xi_k \eta_k.$$